

Research Article

Growth and Characterization of $\text{Ge}_{100-x}\text{Dy}_x$ ($x \leq 2$) Nanowires

K. B. Paul,^{1,2} G. I. Athanasopoulos,¹ C. C. Doumanidis,¹ and C. Rebholz¹

¹Hephaistos Nanotechnology Research Center, University of Cyprus, 75 Kallipoleos Avenue, P.O. Box 20537, 1678 Nicosia, Cyprus

²Advanced Materials Research Institute (AMRI), University of New Orleans, New Orleans, LA 70148, USA

Correspondence should be addressed to K. B. Paul, dr_kpaul@hotmail.com

Received 5 November 2009; Accepted 8 January 2010

Academic Editor: Rosa Lukaszew

Copyright © 2010 K. B. Paul et al. This is an open access article distributed under the Creative Commons Attribution License, which permits unrestricted use, distribution, and reproduction in any medium, provided the original work is properly cited.

Novel semiconducting Germanium-Dysprosium nanowires are fabricated by a combined two-step method, which consists of initial arc-melting of the elemental constituents into a pellet and its heat treatment, followed by thermal vapor transport of the powdered pellet in a tube reactor for fabrication of the nanowires. The nanomaterials are fabricated on gold nucleation seeds on Si/SiO₂ substrates. The thermodynamic conditions in the reactor are carefully chosen to produce wires with diameters in a narrow, specific range. This nanofabrication method ensures high phase purity and crystallinity of nanowires. Based on the results and theoretical work, it is concluded that the fabricated Ge₉₈Dy₂ materials are in a glassy state below 20 K.

1. Introduction

Dilute magnetic semiconductor (DMS) nanowires (NWs) are a topic of intensive investigation [1] due to their possible application in many fields, such as spintronics [2], magnetic sensors [3], and magnetic storage technology [4]. Germanium (Ge) has markedly high semiconductor parameters [5], which indicate prominent quantum size effects, and therefore, promise operative and efficient quantum devices [6]. In Ge-based DMS, Ge is usually doped with a 3D magnetic element: Fe [7, 8], Co [8, 9], Cr [10], and particularly Mn [8, 11, 12], for its ability to initiate room-temperature ferromagnetism [1].

Among the several synthetic strategies for Ge-based magnetic nanowires [12–14], chemical vapor deposition (CVD) [15] is the most popular technique because of its simplicity, low cost, and ease to manipulate the thermodynamic parameters of the process. (When no chemical reaction is involved in the reactor tube, CVD is named thermal vapor transport [15].) This method allows large-scale fabrication of NWs with different sizes on various substrates simultaneously. To achieve homogeneous size and phase in the process of growth, several approaches have been explored, mainly focused on the substrate for the nanowires and the thermodynamic conditions in the reactor [8, 13, 16].

In these studies the structural and morphological parameters of the NWs, such as crystallinity, diameter, and length, were achieved by adjusting the rate of the flowing argon (Ar) gas, the pressure in the reactor tube, the temperature of the powder-source, and the temperature of the substrate with seeds for the NWs.

The concentrations of the dopants in these works were obtained merely by placing the metal precursors at suitable temperatures along the reactor on separate stages [8]. Thus, successive experiments could not reproduce one and the same concentration of the constituents in the wires.

A semiconductor nanodevice is often designed and expected to switch magnetically or electrically and perform as a field-effect transistor. It is well known that the phase purity, presence of alien oxides, and particularly the amorphous oxide-coating on the material may worsen significantly the performance of a device. Works on Ge-based nanowires report on existence of unwanted phases [12, 14] and of an amorphous oxide sheath [8, 16].

The morphology of the nanowires is also tentatively manipulated by attempts to change controllably the size of the nucleation seeds for the nanowires. For example, experiences including ours prove that the diameters of the produced nanowires may vary in a large and random range if the nucleation seeds are sputtered and heat treated on a substrate [16].

In this work, Ge is intermixed with the strong paramagnetic lanthanide Dysprosium (Dy) in search of a new semiconductor, possibly applicable as a DMS at the appropriate concentrations of Dy. Another objective of the work is to describe a route for overcoming part of the above-mentioned problems in the fabrication process. We demonstrate a simple two-step method for preparation of phase-homogeneous semiconducting NWs protected from the oxide on their surfaces. The method is based on fabricating a highly homogeneous bulk pellet before the NW growth. We describe the method and demonstrate examples of the produced GeDy nanowires.

2. Experimental

Appropriate amounts of bulk Ge and Dy (99.995%, Alfa Aesar) were weighted in a glove box for fabrication of a $\text{Ge}_{98}\text{Dy}_2$ alloy. The materials were transported in an Ar atmosphere to an arc-melting furnace. They were remelted three times to prepare an ingot, which served as a base material for the preparation of the NWs. The ingot was heat-treated at 912°C for 20 hours in vacuum for homogenization of the $\text{Ge}_{98}\text{Dy}_2$ alloy.

The powdered material from the ingot, prepared in a glove-box, was separated into two parts. One part was investigated for phase composition and basic magnetic behavior by X-ray diffraction (XRD) and thermoremanent magnetization (TRM) measurements. The second part was transferred in a desiccator under vacuum to a reactor, placed in a Lindberg BlueM Mini Lite tube-furnace for fabrication of the NWs.

The substrates for the nanowires were gold (Au) seeds, produced on commercial $\text{Si}(100)/\text{SiO}_2(300\text{ nm})$ wafers. First, 2 nm-thick Au films were deposited on the wafers by electron-beam evaporation with a deposition rate of 0.2 \AA/s . Then the Au films were heat-treated in vacuum at 500°C for 1 hour to form the Au nucleation seeds for the nanowires.

The nanowires were processed in a quartz tube with length 1 m and diameter 1 inch. The parameters of the deposition process were adjusted according to the dimensions of the reactor tube and the designed thermodynamic process in it: the Ar gas pressure was $2.93 \cdot 10^4\text{ Pa}$, the Ar gas flow-rate was 200 standard cubic centimeters per minute (sccm), the temperature of the GeDy powder source -900°C , the temperature of the Au substrate -500°C , and the deposition time was 10 minutes.

The morphology of the fabricated nanowires was studied with a TESCAN Scanning Electron Microscope (SEM); part of the work was done using a Field Emission SEM (FE-SEM) LEO 1530VP. X-ray energy dispersive (EDX) spectra were measured with a Princeton γ -Tech Sahara II Silicon Drift Detector, which has resolution $\approx 140\text{ eV}$ at 100 kcps. The Transmission Electron Microscope (TEM) images were recorded with a JEOL 2010. The XRD measurements were made with a Philips X'Pert X-ray powder diffractometer.

Magnetic measurements, specifically, thermoremanent magnetization measurements (TRM), were made with a Quantum Design Magnetic Property Measurement System

MPMS-4. Temperature (T) dependence of the TRM (T) was recorded to identify possible alien phases and phase-transitions in the materials. In these measurements the sample is cooled down to 4.2 K in a magnetic field (in the presented results -100 Oe), the field is cut down to zero at the lowest temperature, and the magnetization is measured versus increasing temperature with a step according to expected behavior (5 degrees in these results). At the temperatures of possible phase transition(s), the TRM (T) will exhibit peaks due to a magnetic phase transition. Assumingly, the basic magnetic sublattices have been ordered as the material was cooled down in a magnetic field.

3. Results and Discussion

In Figure 1, the structure and morphology of the produced materials in the utilized conditions of fabrication is displayed. Clusters with an average size $\approx 70\text{ }\mu\text{m}$, situated on the Au seeds on Si/SiO_2 , are created for 10 minutes deposition-time, as observed in Figures 1(a) and 1(b). The details within a cluster can be perceived from Figures 1(c) and 1(d). It is seen that the clusters consist of nanowires, which originate from the Au seeds, and which are headed for all possible directions. The homogeneity of the diameters within a cluster of nanowires is remarkably consistent. In the conditions of the deposition, an average diameter of 30 nm is observed in most clusters of the sample (see e.g., Figure 1(d)).

The generated size of the clusters is dependent on the size of the Au nucleation seeds on the substrate. However, the size of a nanowire inside a cluster is dependent on the thermodynamic conditions in the reactor. It is well known that to generate nanowires on the nuclei, the temperature of the powder-source may vary within a narrow operative temperature range. In these experiments and for these materials (Ge, Ge-3d element, and GeDy), the temperature interval is ≈ 120 degrees, starting from 800°C for Ge-3d element powders [8], and ending at $\approx 920^\circ\text{C}$ when the substance evaporates vigorously without attachment to a substrate due to its high energy. It should be noted also that the temperature of the powder-source is conditional on the state of the powder itself. A fine and uniformly ground powder combined with suitable pressure in the reactor will require a lower and stable temperature within the possible range, to attain sublimation (the solid-vapor-solid process (SVS)) or/and evaporation (the liquid-vapor-solid process (LVS)), and uniform wires.

The temperature of the Au nuclei (T_2) and their distance from the powder-source (L) may affect the quality of the nanowires in a cluster. Ideally, these two factors, T_2 and L , should not be interdependent in order to operate more effectively in a fabrication process. Their independence can be achieved, for example, by using a three zone tube-furnace and tube-reactors of various lengths. The distance from the powder-source has an effect on the morphology of the nanowires. Wires of higher energy (and larger mass) will land on more distant substrates; therefore, the expected diameters and length of the nanowires on a distant Au substrate

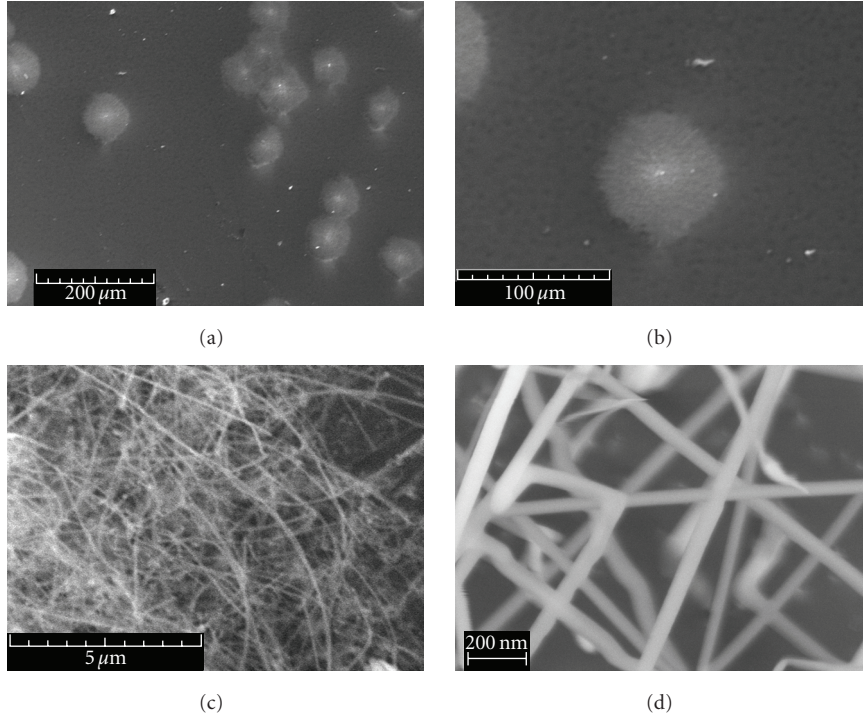


FIGURE 1: A view of the produced material: (a) Clusters of nanowires on Au seeds, (b) One cluster of nanowires, (c) A detailed SEM image inside a cluster. (d) Nanowires of diameter ≈ 30 nm.

are larger, provided that the process is combined with a compatible gas flow-rate. The temperature of the Au nuclei also affects indirectly the morphology of the nanowires by staging on the seeds only material within a specific energy-range. For example, material with higher and incompatible energy will not be accommodated permanently on a stage with nuclei of a particular energy or temperature T_2 .

The quality of the produced nanowires was further examined for presence of oxides, alien phases, alien elements, and morphology. Low-resolution TEM measurements were performed to verify the absence of an oxide sheath on the produced nanowires. A homogeneous nanowire with a diameter of ≈ 30 nm is observed in Figure 2(a), as well as the absence of an oxide shell around it. Many works on nanowires of Ge and Ge-3d elements [8, 12, 16] have registered the presence of such an oxide sheath with a thickness of ≈ 5 nm. Our presented results are consistent with all recorded images from various parts of the fabricated materials. Therefore, they prove in favor of the developed fabrication method, or at least for the applied preventive oxidation measures throughout the work.

A recorded EDX spectrum is presented in Figure 2(b), and in the inset of the figure is displayed a magnified part of the spectrum, relevant for Dy. The quantitative analysis, as well as the spectrum revealed a quantity of Dy in the nanowires (< 2 at %), regardless that the weighted amount of Dy was for a 2 at % composite bulk. We attribute the lost amount of Dy to the aggressive step in the fabrication procedure: the arc-melting and the conditions of the heat treatment of the bulk. Therefore, similar experiments with

Ge and Dy employing the described two-step fabrication procedure will require prudent choice of the time for the heat-treatment, also, possibly an additional amount of Dy to compensate for its high losses during the first stage—preparation of the homogeneous bulk.

XRD diffraction measurements were made on the source-powder and on NW-material peeled off from the substrate. Both XRD patterns were identical. An XRD spectrum of peeled material is presented in Figure 3(a). The measured reflections belong to the Ge face cubic centered (fcc) crystalline phase and the estimated lattice parameter is $a = 0.5661$ nm, very close to the lattice constant of Ge, $a_{\text{Ge}} = 0.5658$ nm (difference of 0.05 %). Therefore, according to the XRD measurements, the nanowires have crystalline structure without secondary phases. Similar lattice parameters, unaffected from the dopant, are reported in reference [8] for Ge-Mn nanowires, with Mn up to 5 at %.

Thermoremanent measurements are frequently used as a sensitive method above the capabilities of XRD to prove the presence of alien phases and phase transitions in various magnetic materials [17]. In Figure 3(b) the temperature dependence of the thermoremanent dc mass magnetic susceptibility, $\chi_{\text{dc}}(T)$, is presented. The plot indicates a paramagnetic behavior above 20 K and a very dilute, disordered, spin-glass-like phase (superparamagnetic) below it. The calculated value of the Curie constant, C , from the relation $\chi_{\text{dc}} = C/T$ at $T > 20$ K, is $\approx 1.81 \times 10^{-3} \text{ m}^3 \cdot \text{K}/\text{kg}$ —approximately two orders of magnitude smaller than cited values for strong magnetic materials [18]. The magnetic susceptibility of this material χ_{dc} at room temperature

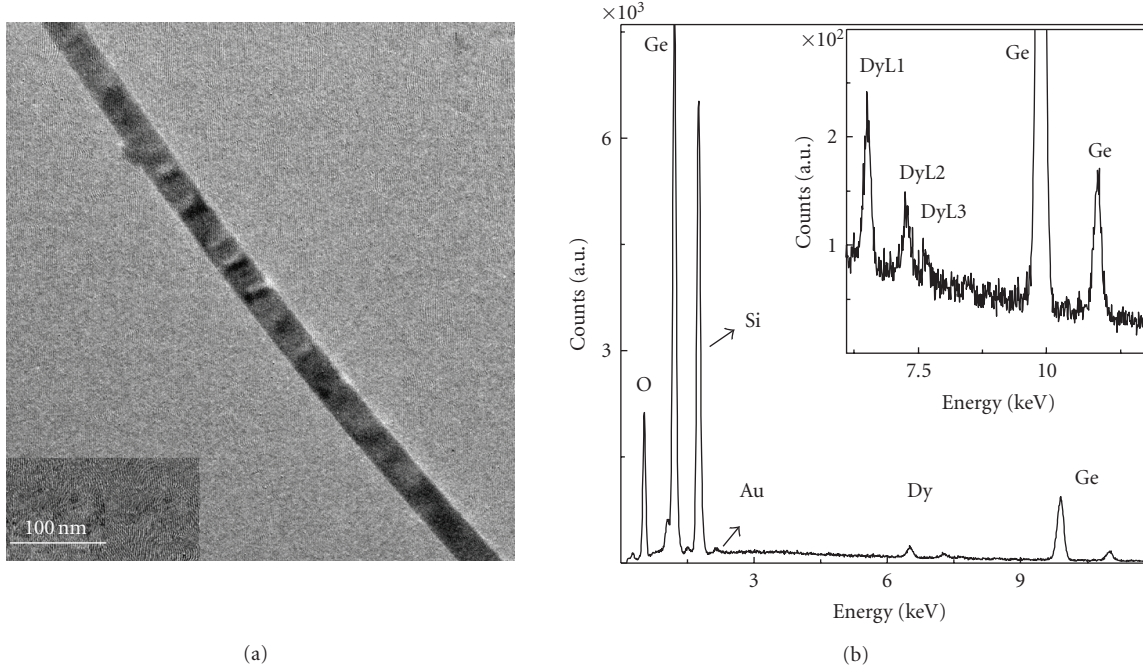


FIGURE 2: (a) A low-resolution TEM image of a $\text{Ge}_{98}\text{Dy}_2$ nanowire. (b) EDX spectrum acquired with an SEM, supplied with a Sahara II Silicon drift detector. In the inset is displayed the magnified part of the spectrum between 6 keV and 12 keV with DyL1, DyL2, DyL3, and GeK-peaks.

is $\approx 5 \times 10^{-6} \text{ m}^3/\text{kg}$, also two orders of magnitude smaller than the χ_{dc} of Dy at room temperature [19].

Dy has a complex magnetic behavior: a strong paramagnetic at room temperature with $\chi_{\text{dc}} \approx 5.9 \times 10^{-4} \text{ m}^3/\text{kg}$, antiferromagnetic between 85 K and 178.5 K, and ferromagnetic below 85 K [19].

Ge is a diamagnetic material with values of the diamagnetic susceptibility dependent on the purity and the doping in the semiconductor [20]. The diamagnetic susceptibility of Ge is temperature-dependent, its absolute value increases up to $\approx 5\%$ upon cooling the undoped semiconductor, and it is $\approx -1.265 \times 10^{-7} \text{ emu/g}$ at room temperature [20]. The absolute value of the susceptibility may increase up to 19 % in an n-type Ge (see e.g., [20] Figures 1, 2, and 4).

The binary Ge-Dy phase diagram [21] specifies a range of ≈ 26 at % of Dy, at which the composite material should be an alloy, possibly in one of the states: from a strong paramagnetic to the ferromagnetic phase [22, 23]. There are no references in the literature at present for the magnetic Ge-Dy phase diagram between 1 and 26 at % of Dy. We aimed at producing $\text{Ge}_{98}\text{Dy}_2$ nanowires. Due to the time interval of the heat-treatment of the bulk (20 h), a part of Dy has presumably been lost. The quantity of Dy left still influences significantly the quality of the general magnetic behavior of Ge as evidenced by Figure 3(b). Thus, it seems viable that at an appropriate concentrations of Dy (e.g. ≤ 10 at %), the materials and the nanowires will exhibit a well-developed, at least soft-ferromagnetic state with considerable coercivity and remnant magnetization at room temperature. In support of this assumption, we refer to reference [24], in which is proved that there is a limited range of magnetic impurity-concentrations (n_i) in a DMS, in which ferromagnetic (FM)

ordering is possible. The clustering of the impurities may shift the FM range to lower concentrations. The Curie temperatures, T_c , are nonmonotonic functions of n_i and have their highest values at $n_i \approx 0.1$ (10%) [24].

Another work [23] on the magnetic phase diagram of disordered dilute magnetic semiconductors predicts ferromagnetism when $n_c/n_i < 1$ (n_c is the concentration of the carriers of the interaction (electrons or holes)). Both works [23, 24] utilize the model of indirect exchange interaction (RKKY) between the magnetic impurities.

Dy in a pure Ge matrix may act as both, an impurity and a donor (creator) of holes. According to reference [23], a DMS with magnetic impurities can be in one of the two states: nonferromagnetic (NFM) or ferromagnetic (FM). The boundary between the NFM and the FM phases of the magnetic phase diagram constitutes the line of the magnetic percolation transition [23]. The NFM phase is described as a subtle glassy phase [23]. The expected FM state is characterized as fragile, and depending on the damping of the RKKY-interaction and the balance in n_c/n_i [23].

A larger n_c/n_i is associated with strong antiferromagnetic interactions, which prevent many pairs of spins from aligning. As n_c/n_i drops, small correlated groups of spins may increase in size. Ultimately, the magnetic clusters span the entire system and magnetic percolation occurs, signaling the appearance of a long-range FM order. In the nanoscale, in the NFM phase the normalized correlation length ζ/L increases as the size of the object, L , decreases. For FM order, ζ/L decreases when reducing L [23]. Accordingly, it is more difficult to observe the FM state in one-dimensional materials.

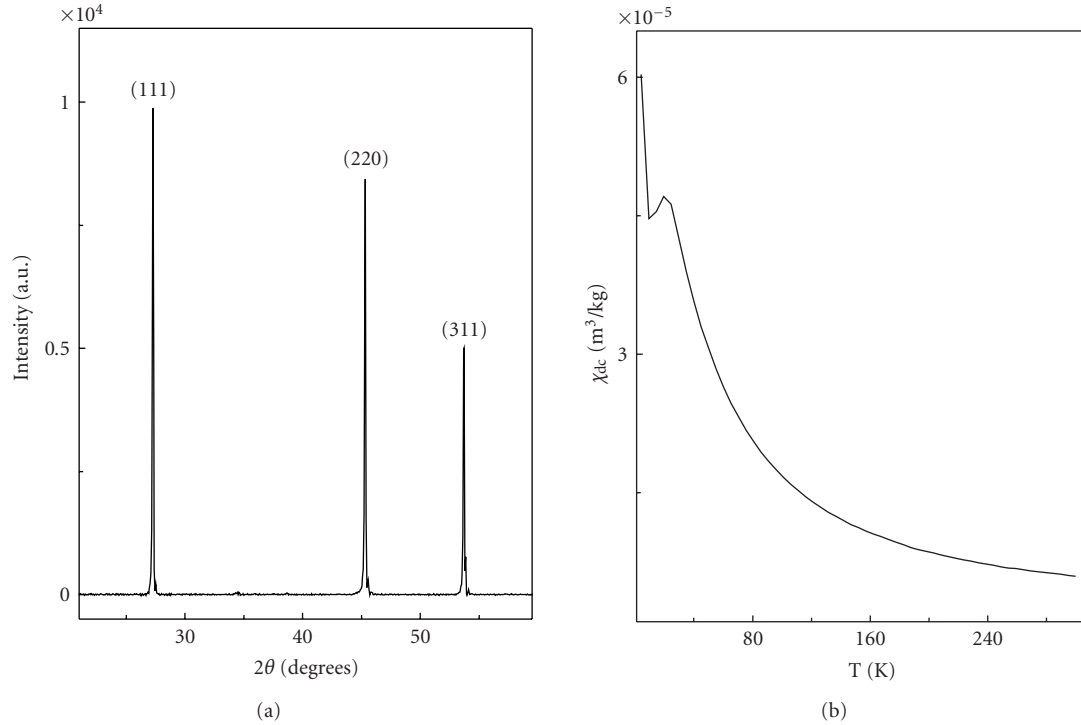


FIGURE 3: (a) XRD pattern of NW material. (b) TRM (T).

In reference [25] it is argued that in the case of a random distribution of magnetic ions, delocalized or weakly localized holes in the valence band are necessary to promote ferromagnetism, characterized by Curie temperatures ≥ 20 K. This result is supportive to our conclusion that the fabricated materials are in a glassy state below 20 K, possibly, close to the percolation boundary.

4. Conclusions

An experimental pathway to fabricating highly homogeneous, crystalline, alloy $Ge_{100-x}Dy_x$ nanowires with various concentrations of Dy is outlined in the work.

The materials are unexplored in both, bulk and one-dimensional form, and the results are encouraging to proceed with higher concentrations of Dy to determine the magnetic phase diagram and one-dimensional behavior of various entities of this material.

We showed that using a combined two-step solid state method based on arc-melting of the ingredients and thermal vapor transport, highly homogeneous $Ge_{98}Dy_2$ nanowires can be formed. According to XRD, SEM, and TEM measurements the formed wires are crystalline and have a diameter ≈ 30 nm and an average length of $5 \mu m$ on the as-prepared substrate, and in the thermodynamic conditions in the tube reactor. Our experimental results on magnetic behavior in very low magnetic fields, as well as theoretical work [23–25], support the conclusion that the fabricated nanowires are NFM for $Dy \leq 2$ at %. Future work on higher concentrations of Dy (≤ 10 at %) will shed light on the magnetic phase diagram of this material in one-dimensional form.

Acknowledgments

The authors acknowledge the European Commission for funding this project under grant Marie Curie Excellence Team - NanoHeaters EXT-0023899 and ICT 224596. They gratefully acknowledge the funding support from the Cypriot Research Promotion Foundation—*NanoCyprus*. The authors would like also to thank Mr. Jim Garrett from Brockhouse Institute at McMaster University in Hamilton, Canada for helpful discussions on the maintenance of these materials.

References

- [1] J. S. Kulkarni, O. Kazakova, and J. D. Holmes, "Dilute magnetic semiconductor nanowires," *Applied Physics A*, vol. 85, no. 3, pp. 277–286, 2006.
- [2] H. Ohno, "Making nonmagnetic semiconductors ferromagnetic," *Science*, vol. 281, no. 5379, pp. 951–956, 1998.
- [3] C. Schott, F. Burger, H. Blanchard, and L. Chiesi, "Modern integrated silicon Hall sensors," *Sensor Review*, vol. 18, no. 4, pp. 252–257, 1998.
- [4] S. X. Wang and A. M. Taratorin, *Magnetic Information Storage Technology: A Volume in the Electromagnetism Series*, Academic Press, New York, NY, USA, 1999.
- [5] Y. Maeda, N. Tsukamoto, Y. Yazawa, Y. Kanemitsu, and Y. Masumoto, "Visible photoluminescence of Ge microcrystals embedded in SiO_2 glassy matrices," *Applied Physics Letters*, vol. 59, no. 24, pp. 3168–3170, 1991.
- [6] J. Xiang, W. Lu, Y. Hu, Y. Wu, H. Yan, and C. M. Lieber, "Ge/Si nanowire heterostructures as high-performance field-effect transistors," *Nature*, vol. 441, no. 7092, pp. 489–493, 2006.

- [7] R. Goswami, G. Kioseoglou, A. T. Hanbicki, O. M. J. van 't Erve, B. T. Jonker, and G. Spanos, "Growth of ferromagnetic nanoparticles in Ge:Fe thin films," *Applied Physics Letters*, vol. 86, no. 3, Article ID 032509, 3 pages, 2005.
- [8] Y. J. Cho, C. H. Kim, H. S. Kim, et al., "Ferromagnetic $\text{Ge}_{1-x}\text{M}_x$ ($M = \text{Mn}, \text{Fe}, \text{and Co}$) nanowires," *Chemistry of Materials*, vol. 20, no. 14, pp. 4694–4702, 2008.
- [9] T. A. Crowley, B. Daly, M. A. Morris, et al., "Probing the magnetic properties of cobalt-germanium nanocable arrays," *Journal of Materials Chemistry*, vol. 15, no. 24, pp. 2408–2413, 2005.
- [10] S. Choi, S. C. Hong, S. Cho, et al., "Ferromagnetic properties in Cr, Fe-doped Ge single crystals," *Journal of Applied Physics*, vol. 93, no. 10, pp. 7670–7672, 2003.
- [11] S. Cho, S. Choi, S. C. Hong, et al., "Ferromagnetism in Mn-doped Ge," *Physical Review B*, vol. 66, no. 3, Article ID 033303, 3 pages, 2002.
- [12] M. I. van der Meulen, N. Petkov, M. A. Morris, et al., "Single crystalline $\text{Ge}_{1-x}\text{Mn}_x$ nanowires as building blocks for nanoelectronics," *Nano Letters*, vol. 9, no. 1, pp. 50–56, 2009.
- [13] A. R. Phani, V. Grossi, M. Passacantando, L. Ottaviano, and S. Santucci, "Growth of Ge nanowires by chemical vapour deposition technique," in *Proceedings of the NSTI Nanotechnology Conference and Trade Show (Nanotech '06)*, vol. 3, chapter 2, pp. 141–144, 2006.
- [14] R. Morgunov, Y. Tanimoto, and O. Kazakova, "Microwave magnetoresistance in Ge:Mn nanowires and nanofilms," *Science and Technology of Advanced Materials*, vol. 9, no. 2, pp. 24207–24211, 2008.
- [15] J. E. Crowell, "Chemical methods of thin film deposition: chemical vapor deposition, atomic layer deposition, and related technologies," *Journal of Vacuum Science and Technology A*, vol. 21, no. 5, pp. S88–S95, 2003.
- [16] G. Gu, M. Burghard, G. T. Kim, et al., "Growth and electrical transport of germanium nanowires," *Journal of Applied Physics*, vol. 90, no. 11, pp. 5747–5751, 2001.
- [17] E. Lahderanta, K. Eftimova, and R. Laiho, "Magnetic phase diagram and dynamics of low-temperature magnetic behaviour of the $\text{CoAl}_{1-x}\text{Cu}_x$ system," *Journal of Magnetism and Magnetic Materials*, vol. 139, no. 1-2, pp. 189–196, 1995.
- [18] H. P. J. Wijn and R. Poerschke, Eds., *Magnetic Properties of Metals, D-Elements, Alloys and Compounds*, Data in Science and Technology, Springer, Berlin, Germany, 1991.
- [19] D. R. Behrendt, S. Legvold, and F. H. Spedding, "Magnetic properties of dysprosium single crystals," *Physical Review*, vol. 109, no. 5, pp. 1544–1547, 1958.
- [20] D. K. Stevens, J. W. Cleland, J. H. Crawford, and H. C. Schweinler, "Magnetic susceptibility of germanium," *Physical Review*, vol. 100, no. 4, pp. 1084–1093, 1955.
- [21] T. B. Massalski and H. Okamoto, Eds., *Binary Alloy Phase Diagrams*, vol. 2, ASM International, New York, NY, USA, 1986.
- [22] K. Eftimova, R. Laiho, and E. Lahderanta, "On the re-entrant state of the $\text{Pd}_{11}\text{Co}_{50}\text{Al}_{39}$ alloy," *Physica Status Solidi (B)*, vol. 220, no. 2, pp. 969–977, 2000.
- [23] D. J. Priour Jr. and S. Das Sarma, "Phase diagram of the disordered RKKY model in dilute magnetic semiconductors," *Physical Review Letters*, vol. 97, no. 12, Article ID 127201, 4 pages, 2006.
- [24] E. Z. Meilikhov, "Diluted magnetic semiconductors with correlated impurities: mean-field theory with RKKY interaction," *Physical Review B*, vol. 75, no. 4, Article ID 045204, 5 pages, 2007.
- [25] T. Dietl, "Origin of ferromagnetic response in diluted magnetic semiconductors and oxides," *Journal of Physics: Condensed Matter*, vol. 19, no. 16, Article ID 165204, 15 pages, 2007.



Hindawi

Submit your manuscripts at
<http://www.hindawi.com>

